Synthesis and photocatalytic performance of TiO_2 nanospheres–graphene nanocomposite under visible and UV light irradiation

Malgorzata Wojtoniszak, Beata Zielinska, Xuecheng Chen, Ryszard J. Kalenczuk & Ewa Borowiak-Palen

Journal of Materials Science
Full Set - Includes `Journal of Materials Science Letters'

ISSN 0022-2461
Volume 47
Number 7

J Mater Sci (2012) 47:3185-3190
DOI 10.1007/s10853-011-6153-9

Springer

J Mater Sci (2012) 47:3185–3190
DOI 10.1007/s10853-011-6153-9

Synthesis and photocatalytic performance of TiO_2 nanospheres–graphene nanocomposite under visible and UV light irradiation

Malgorzata Wojtoniszak · Beata Zielinska · Xuecheng Chen · Ryszard J. Kalenczuk · Ewa Borowiak-Palen

Received: 7 October 2011 / Accepted: 23 November 2011 / Published online: 6 December 2011

Abstract In this article, we present a fast and simple method to produce TiO_2 nanospheres–graphene nanocomposite with high photocatalytic activity under visible and UV light irradiation. TiO_2 nanospheres were adsorbed on graphene in sol–gel process. First, titanium (IV) butoxide underwent hydrolysis in graphene oxide (GO) ethanol solution resulting in TiO_2 nanospheres deposition on GO. Next, the material was calcinated to generate the phase transition of TiO_2 into anatase and reduce GO to graphene. The detailed characterization of the material was performed via transmission electron microscopy, energy dispersive X-rays spectrometer, Fourier-transformed infrared spectroscopy, X-ray diffraction, and Raman spectroscopy. Interestingly, the band-gap energy of the prepared photocatalyst was drastically decreased in comparison with the commercial photocatalyst P25 from 3.05 to 2.36 eV. This influenced in the activation of the material under visible light and resulted in high photocatalytic activity in the process of phenol decomposition in visible and UV irradiation.

Introduction

Graphene is a flat monolayer of carbon atoms tightly packed into a two-dimensional (2D) honeycomb lattice [1]. Because of its unique electrical, mechanical, and thermal properties, this novel material is expected to be applicable in many areas like electronic devices, nanocomposites, or nanomedicine [2–8]. Furthermore, chemically modified graphene, like graphene oxide (GO), generates a great interest in materials science. Recently, Rourke et al. [9] presented a new point of view concerning a structure of GO. They suggested that oxidative moieties are noncovalently attached to GO. Moreover, Wilson et al. [10] stated that a carbon substructure of GO is found on average to maintain the hexagonal symmetry, order, and carbon–carbon bond length of an unmodified graphene sheet. These observations suggest that models for the structure of GO need revisiting.

Recently, lots of reports on the preparation of TiO_2–graphene (TiO_2–G) or TiO_2–GO nanocomposite and its applications in the photocatalytic reactions have been reported. For example, Jiang et al. [11] synthesized GO/TiO_2 composites by in situ deposition of TiO_2 nanoparticles on GO nanosheets by a liquid phase deposition, and then calcination at 200 °C. The produced composites exhibited higher photocatalytic activity than commercial TiO_2 P25 in the reaction of methyl orange decomposition. High photocatalytic efficiency of GO–TiO_2 composite was attributed to a thin 2D sheet support, a large surface area, much increased adsorption capacity, and a good transfer of photo-generated electrons from the conduction band of TiO_2 to the GO sheet. Liang et al. [12] also stated that TiO_2 nanocrystals on GO show superior photocatalytic activity in comparison to the TiO_2 P25 in the degradation of rhodamine. Zhang et al. [13] studied the photocatalytic activity of TiO_2 P25/graphene composite produced in thermal reaction of GO in the reaction of methylene blue decomposition under visible light irradiation. In this study, the authors point out that TiO_2 P25/graphene exhibits extremely higher photocatalytic activity than pure TiO_2 P25. For the TiO_2 P25/graphene and TiO_2 P25, 70% and only 10% of methylene blue were decomposed after 5 h visible light irradiation, respectively. In these reports [11–13], the

M. Wojtoniszak (✉) · B. Zielinska · X. Chen · R. J. Kalenczuk · E. Borowiak-Palen
Institute of Chemical and Environment Engineering, Westpomeranian University of Technology in Szczecin, Pulaskiego 10, 70-322 Szczecin, Poland
e-mail: mwojtoniszak@zut.edu.pl

respective authors present the photocatalytic activity of TiO_2/graphene nanocomposites, where Titania forms into nanocrystals with diameters ranging from 15 to 40 nm. However, in our study, TiO_2 takes a spherical shape and forms a nanocomposite with graphene.

In this study, TiO_2–G was synthesized by the process of hydrolysis of TBT in the presence of GO ethanol solution resulting in TiO_2 nanospheres deposition on GO. Next, the material was calcinated to induce the phase transition of TiO_2 into anatase and reduction of GO into graphene. The photocatalytic activity of the resulting material was examined during the process of phenol decomposition under UV and visible light irradiation.

Experimental section

TiO_2–G nanocomposite preparation

GO was produced using modified Hummers method, according to [14] and then dispersed in ethanol in concentration of 1 mg/mL. Next, a 10% TBT ethanol solution was mixed with GO ethanol dispersion in the volume ratio of 1:4. The obtained suspension was ultrasonicated (Sonic Ruptor 400, OMNI INTERNATIONAL The Homogenizer Company) and stirred simultaneously for 90 min. After this step, the solution was stirred for 20 h at room temperature. Next, the suspension was centrifuged (9000 rpm, 1 h) to retrieve the sediment. In order to remove excess of titanium dioxide, the sediment was multiple times ultrasonicated and stirred in ethanol for 1 h and centrifuged again (9000 rpm, 1 h). Finally, the material was calcinated in vacuum ($p = 10^{-4}$ mbar) at 400 °C for 2 h to form TiO_2 in anatase phase to reduce GO into graphene.

Photocatalytic activity of TiO_2–G nanocomposite under UV light irradiation

Photocatalytic activity of the nanocomposite was examined in the process of photocatalytic phenol decomposition and was compared to the activity of TiO_2 P25 (Degussa). The photocatalytic reactions were carried out in an open system with the inner-irradiation-type. A medium pressure mercury lamp of 150 W as a light source was applied. The lamp provided light of wavelength ranging from 200 to 600 nm with the maximum intensity of 366 nm. In a typical procedure of the reaction, 300 mg of a catalyst (TiO_2/graphene or TiO_2 P25) was dispersed in a 600 mL of phenol solution with starting concentration of 10 mg/mL and next, poured into the reactor followed by stirring in darkness for 15 min (for adsorption of phenol onto photocatalyst surface). Then, the lamp was turned on and the mixture was irradiated for 2 h.

Photocatalytic activity of TiO_2–G nanocomposite under visible light irradiation

The photoactivity of TiO_2–G under visible light irradiation was also studied in the process of phenol decomposition and was compared to TiO_2 P25. Here, 100 mg of a photocatalyst was dispersed in a 300 mL of phenol solution with starting concentration of 5 mg/mL. The lamp provided light of wavelength ranging from 400 to 900 nm with the maximum intensity of 650 nm. During the processes, the samples were taken from the mixture in regular time intervals to determine the concentration of phenol in the reaction solution using UV–Vis spectroscopy with a calibrated curve at the wavelength 270 nm.

Characterization

The morphology and chemical composition of the samples were examined using high resolution transmission electron microscopy (TEM, Tecnai F30)—in both, bright field image and high-angle annular dark field, and its energy dispersive X-ray (EDX) spectrum were obtained. FT-IR absorption spectra were recorded on Nicolet 6700 FT-IR Spectrometer. Raman spectra were performed using in Via Raman Microscope (Renishaw), with the excitation wavelength of 785 nm. X-ray diffraction (XRD) patterns were carried out using X'Pert Philips Diffractometer with Cu anode ($K_{\alpha 1} = 1.54056$ Å) to investigate crystal composition of the samples. UV–Vis absorption spectra of phenol solution were recorded in Jasco V-570 UV–Vis spectrometer to determine degree of phenol decomposition during photocatalytic process. The optical properties of the materials were investigated by means of the diffuse reflectance (DR) UV–Vis technique, using a Jasco (Japan) spectrometer.

Results and discussion

Morphology and structure of the TiO_2–G photocatalyst

Morphology and elemental composition of TiO_2–G nanocomposite were investigated using transmission electron microscopy, HAADF, and energy dispersive X-ray analysis. According to the TEM (Fig. 1a) analysis, it was found that diameters of the nanospheres adsorbed on the surface of graphene ranged from 100 to 250 nm and the dominating fraction of the nanospheres was $\sim$200 nm. Figure 1b presents EDX spectrum collected from the area presented in Fig. 1. It clearly demonstrates the composition of the sample: Ti, O, and C. Moreover, more detailed elemental analysis has been performed. The profile composition presented in Fig. 1d was collected along the red

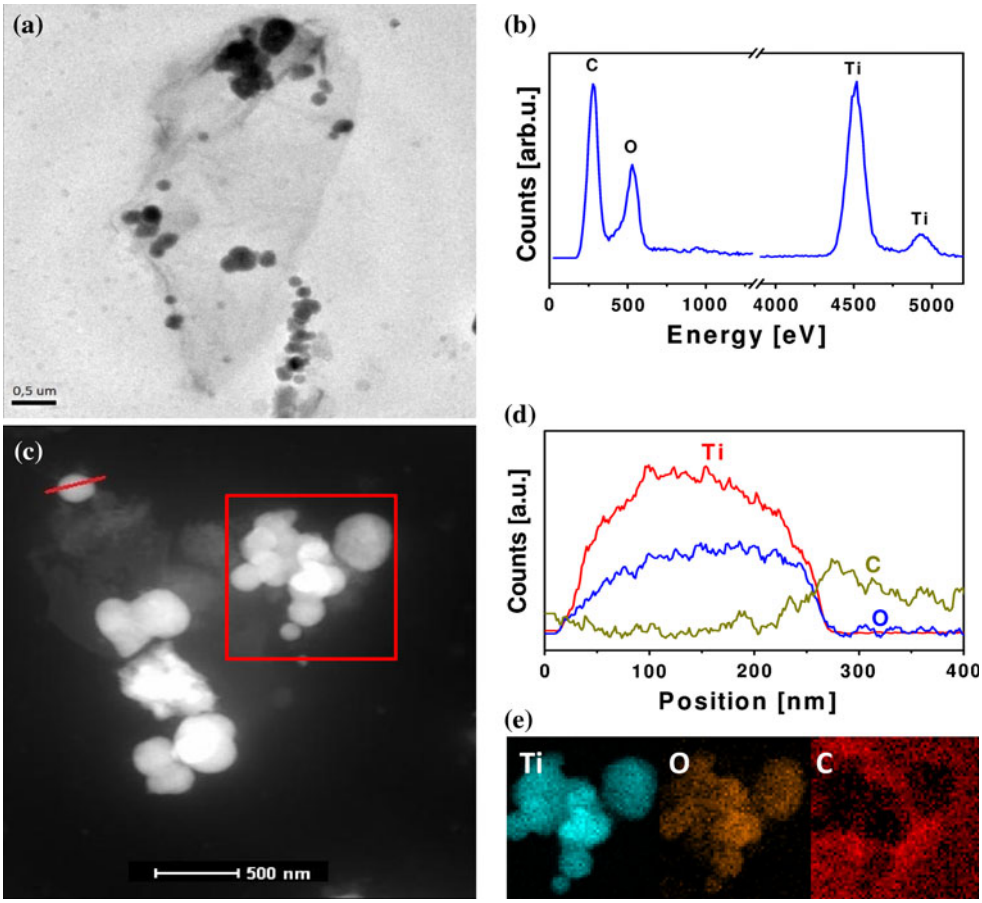

Fig. 1 **a** TEM and **c** STEM images of TiO_2–G nanocomposite with EDX spectrum obtained from bulkscale analysis (**b**), **d** EDX scanning corresponding to the profile in the image (**c**), **e** EDX mapping corresponding to the square-area in the image (**b**) showing the distribution of titanium (*left image*), oxygen (*middle image*) and carbon (*right image*)

line presented in STEM image (Fig. 1c). The signals of Ti and O increase simultaneously when the signal from nanosphere is collected, whereas the carbon signal appears when the signal comes from the supporting material. Furthermore, basing on the same STEM image, the elemental mapping has been performed (Fig. 1e). This clearly demonstrates the distribution of the Ti, O, and C confirming the sample composition on a local scale.

In order to confirm the sample composition in a bulk scale, two characterization tools have been used: Raman spectroscopy (Fig. 2a) and XRD (Fig. 2b). Figure 2a shows Raman spectra of GO and TiO_2–G. The first spectrum exhibits two main peaks, at 1315 and 1593 cm^{-1}, named as D band and G band, respectively. The D band is a breathing mode of A_{1g} symmetry involving phonons near the *K* zone boundary [15, 16]. The G band originates from in-plane vibration of sp^2 carbon atoms and is a doubly degenerate phonon mode (E_{2g} symmetry) at the Brillouin zone center [17–19]. These peaks are also present at TiO_2–G spectrum. In addition, the spectrum exhibits six active modes corresponded to anatase crystal. The peaks arise in the following positions: 152 cm^{-1} (E_g), 203 cm^{-1} (E_g), 302 cm^{-1} (B_{1g}), 395 cm^{-1} (B_{1g}), 508 cm^{-1} (A_{1g}), and 634 cm^{-1} (E_g) [20]. Raman spectroscopy confirms synthesis of GO and next anatase–TiO_2 nanospheres deposition on graphene. This was fully acknowledged by XRD. Here, GO pattern is dominated by single peak at 10375° (001). TiO_2–G XRD pattern exhibits diffraction peaks at 25°(101), 37°(103), 38°(004), 39°(112), 48°(200), 54°(105), 55° (211), 63° (118), 69° (116), and 70° (220). These peaks are related to anatase crystalline form of TiO_2 nanocrystals deposited on graphene [21].

Furthermore, we determined the content of graphene in the prepared photocatalyst via thermogravimetric analysis (data not presented here). It was found that approximately 5% of graphene is present in TiO_2–G.

In order to characterize the structure of the received TiO_2–G photocatalyst, we used FT-IR spectroscopy. Figure 3 shows FT-IR spectra of GO and TiO_2–G. GO exhibits the following absorption modes: at 1090 cm^{-1} attributed to the C–O stretching vibration mode in the alkoxy group, at 1620 cm^{-1} due to C=C aromatic bonding; at 1160 cm^{-1} corresponding to the epoxy C–O stretching peak; at 1450 cm^{-1} arising from the C–OH carboxyl group; at 1725 cm^{-1} related to the C=O stretch mode in the carboxyl group; and at 3430 nm from O–H groups [22]. Subsequently, the spectrum of TiO_2–G has changed significantly. In this study, each absorption mode attributed to

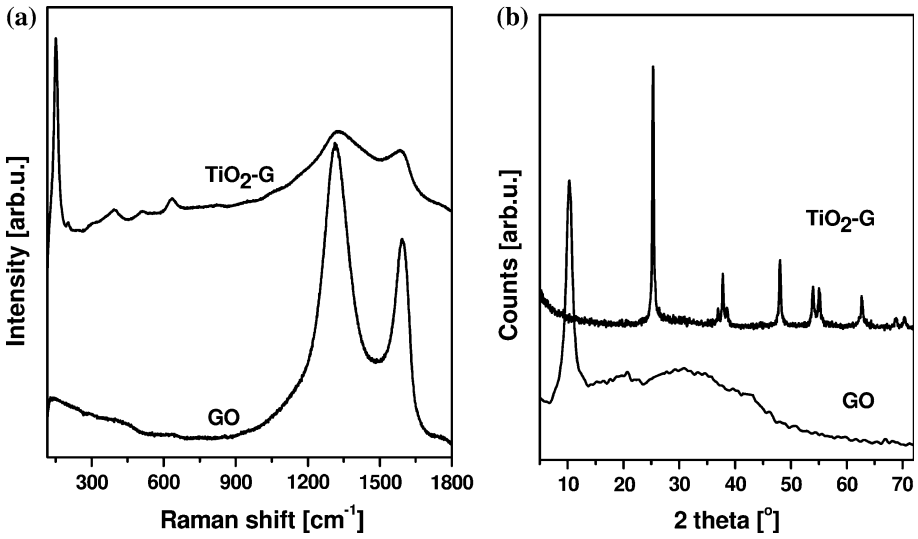

Fig. 2 Raman spectra (**a**) and XRD patterns (**b**) of graphene oxide (*GO*) and TiO_2–G

the functional groups disappears indicating complete reduction of GO, and three strong peaks appear at 621, 652, and 679 cm^{-1} because of Ti–O–Ti group [23]. Moreover, a peak at 1130 cm^{-1} is observed which is ascribed to the vibration of Ti–O–C bond [24, 25]. This indicates that titanium dioxide nanospheres are chemically bounded to graphene. TiO_2–G spectrum exhibits a peak at 1631 cm^{-1} corresponding to C=C aromatic bond arising from graphene.

DR–UV–Vis analysis

For estimate the band gap energy of TiO_2–graphene nanocomposite and TiO_2 P25 the optical analysis were conducted. The DR–UV–vis spectra of the studied samples are presented in Fig. 4a. From this figure, it is clearly seen that the absorption edge of TiO_2–G is shifted towards longer wavelength in comparison to the TiO_2 P25. To determine the band gap energy, the Kubelka–Munk method based on the diffuse reflectance spectra was employed. The experimental details were given earlier [26]. Figure 4b plots the relationship of $[F(R)hv]^{1/2}$ versus photon energy (hv). The estimated band gap energy of TiO_2 P25 and TiO_2–G is 3.05 and 2.36 eV, respectively. This phenomenon is related to chemical bonding between titanium dioxide and graphene what was confirmed by FT-IR spectroscopy. Therefore, the photocatalytic activity of TiO_2–G was examined under UV and visible light irradiation and was compared with the commercial P25.

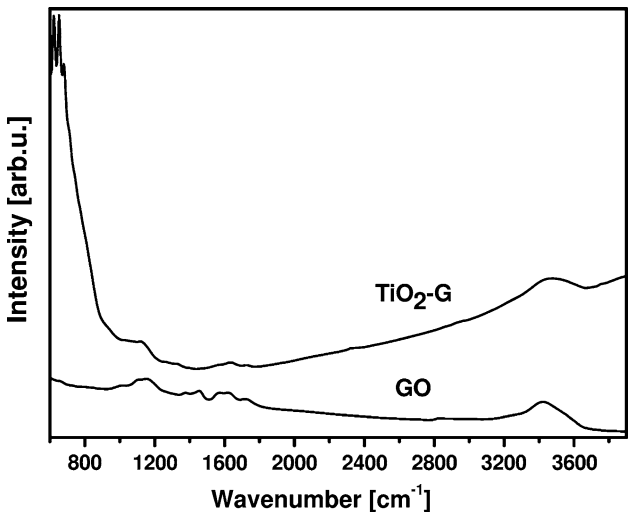

Fig. 3 FT-IR spectra of GO and TiO_2–G

Photocatalytic reactions

Phenol was selected as a model organic pollutant to study the photocatalytic performance of the TiO_2–G nanocomposite. The TiO_2–G was compared in respect to equivalent studies with commercial TiO_2 P25. The results of the photocatalytic phenol decomposition under UV light are shown in Fig. 5. It presents a plot of C/C_0 versus time (t), where C is concentration of the phenol at the certain time and C_0 is initial concentration of phenol (mg/L). Here, TiO_2–G nanocomposite is an active photocatalyst for phenol decomposition. Moreover, TiO_2–G possesses the similar photocatalytic activity in phenol decomposition in comparison to the TiO_2 P25. For example, after 100 min of UV irradiation, 95 and 91% of phenol decomposition was obtained for TiO_2 P25 and TiO_2–G, respectively.

Furthermore, it is known that the photocatalytic activity of photocatalysts strongly depends on pH of the reaction mixture. Yuan et al. [27] stated that the optimum activity of the pure TiO_2 in the reaction of phenol decomposition

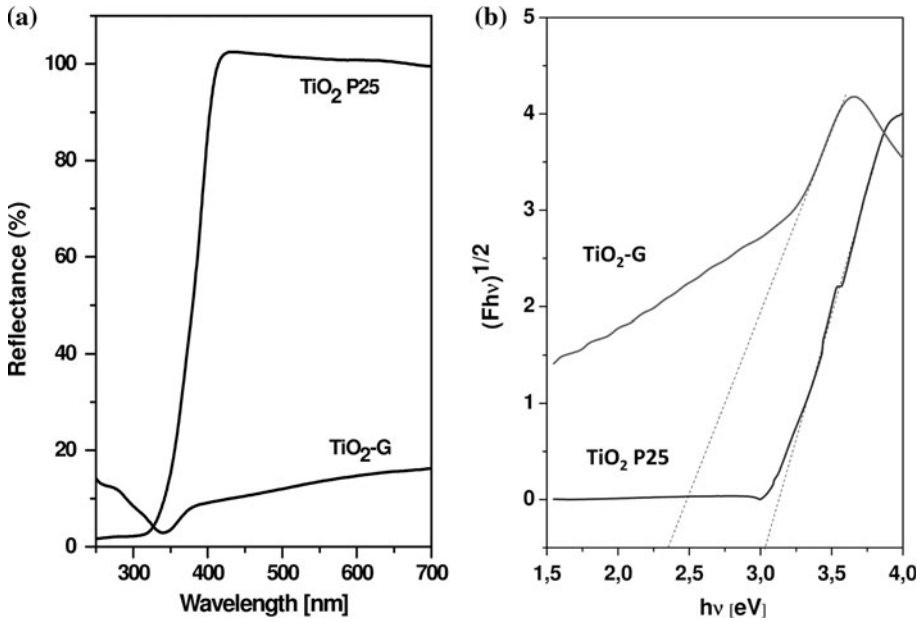

Fig. 4 **a** DR–UV–Vis spectra and **b** Kubelka–Munk plot for band gap evaluation of studied materials (TiO_2–P25 and TiO_2–graphene)

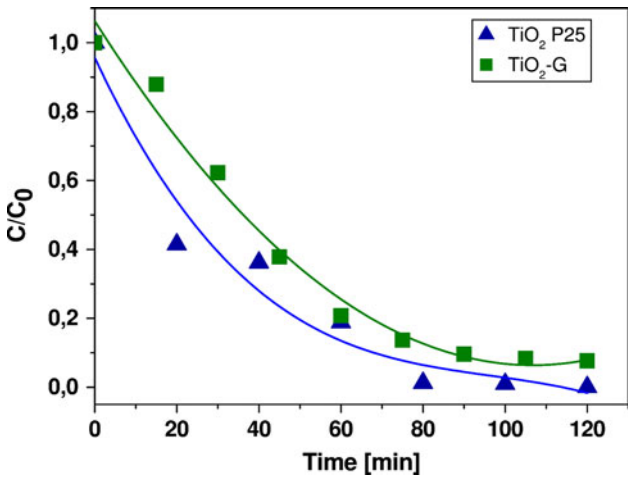

Fig. 5 Photocatalytic phenol decomposition under UV light irradiation on the TiO_2–P25 and TiO_2–G–phenol concentration 10 mg/dm^3, initial pH—6.7

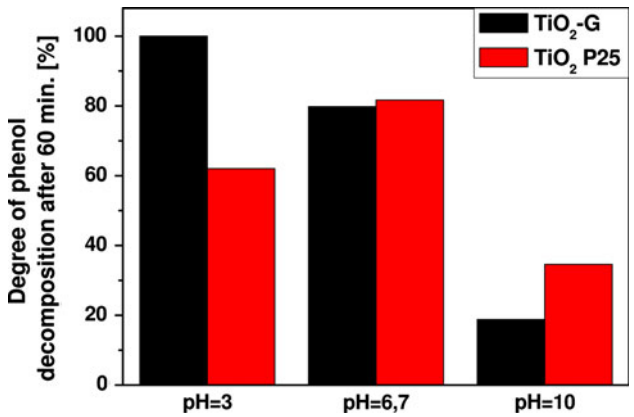

Fig. 6 Comparison of TiO_2–G and P25 photocatalysts activity depending on pH. The graph presents degree of phenol decomposition after 60 min of UV light irradiation

occurs at pH 3–4. Therefore, the photocatalytic decomposition of phenol at pH 3, 6.7, and 10 was also studied. The results are shown in Fig. 6, which present a degree of phenol decomposition after 60 min of UV light irradiation. In this case, it is clearly shown that the activity of the catalysts decreases when pH is increased. Interestingly, TiO_2–G nanocomposite exhibits similar photocatalytic performance to the commercial P25. However, the reactivity of our system drastically increased at pH 3. The enhancement of phenol degradation in the acidic pH can be explained by the minimalization of electron–hole pairs' recombination [28]. This high photocatalytic activity of TiO_2–G can be due to graphene possessing remarkable electronic transport properties. In TiO_2–G nanocomposite, the excited electrons can be quickly transferred from the conduction band of TiO_2 to the surface of graphene, improving the separation of the electron–hole pairs and also the photocatalytic efficiency [13].

Finally, we performed the examination of photocatalytic activity of TiO_2–G nanocomposite under visible light irradiation. It was compared with the commercial photocatalyst TiO_2 P25. The results are presented in Fig. 7. It was observed that within 20 h, the photocatalysts exhibit similar photocatalytic performance under visible light, but interestingly, after 24 h, the P25 underwent deactivation (~42% of phenol was not decomposed) while the reaction in the presence of TiO_2–G lasted 96 h (~7% of phenol was not decomposed). The higher activity of the prepared nanocomposite is related to the electronic interaction between TiO_2 and graphene which resulted in the reduction

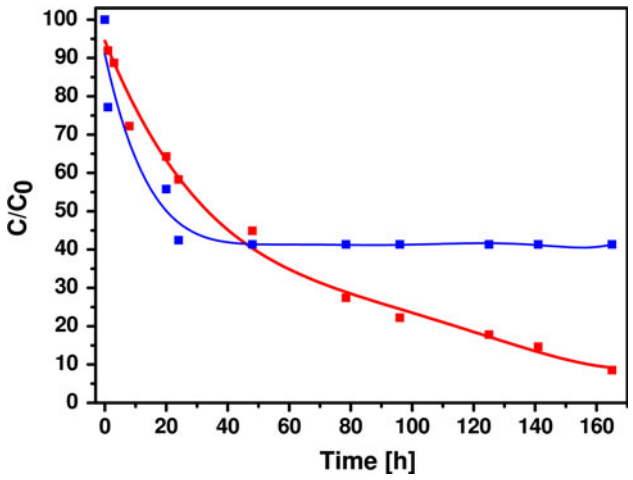

Fig. 7 Photocatalytic phenol decomposition under visible light irradiation on the TiO_2–P25 and TiO_2–G—phenol concentration 5 mg/dm^3

of band-gap energy to 2.36 eV. Under visible light irradiation, the photogenerated electrons of TiO_2 nanospheres transferred quickly to graphene which inhibited the charge recombination and promoted the photocatalytic activity of the material. Furthermore, the exceptional electron mobility of graphene increased the charge transport rate and enhanced electron–hole pairs separation.

Conclusions

In summary, we have successfully synthesized TiO_2 nanospheres adsorbed on graphene with fast and simple methodology. A band-gap energy of the material drastically decreased from 3.05 to 2.36 eV because of electronic interaction between TiO_2 and graphene, in comparison with the commercial photocatalyst TiO_2 P25. This phenomenon resulted in high photocatalytic performance under visible light irradiation in the process of phenol decomposition. The photocatalytic activity was also investigated under UV light irradiation depending on pH. It was found that the activity of the material increased when pH was decreased, and significantly exceeded the performance of P25 when pH was set to 3. These results open up a new opportunity to produce titania-based materials in the application of photocatalysis, water treatment, and others.

Acknowledgement The authors are grateful for the financial support received from the Foundation for Polish Science under FOCUS 2010 Program.

References

1. Novoselov KS, Geim AK, Morozov SV, Jiang D, Zhang Y, Dubonos SV et al (2004) Science 306:666. doi:10.1126/science.1102896
2. Lee C, Wei X, Kysar JW, Hone J (2008) Science 321:385. doi:10.1126/science.1157996
3. Balandin AA, Ghosh S, Bao W, Calizo I, Teweldebrhan D, Miao F et al (2008) Nano Lett 8:902. doi:10.1021/nl0731872
4. Chen JH, Jang C, Xiao S, Ishigami M, Fuhrer MS (2008) Nat Nanotechnol 3:206. doi:10.1038/nnano.2008.58
5. Fowler JD, Allen MJ, Tung VC, Yang Y, Kaner RB, Weiller BH (2009) ACS Nano 3:301. doi:10.1021/nn800593m
6. Liang M, Zhi L (2009) J Mater Chem 19:5871. doi:10.1039/B901551E
7. Ramanathan T, Abdala AA, Stankovich S, Dikin DA, Herrera-Alonso M, Piner RD et al (2008) Nat Nanotechnol 3:327. doi:10.1038/nnano.2008.96
8. Yang K, Wan J, Zhang S, Zhang Y, Lee ST, Liu Z (2011) ACS nano 5:516
9. Rourke JP, Pandey PA, Moore JJ, Bates M, Kinloch IA, Young RJ, Wilson RN (2011) Angewandt Chem-Int Ed 50:3173. doi:10.1002/anie.201007520
10. Wilson NR, Pandey PA, Beanland R, Young RJ, Kinloch IA, Gong L, Liu Z, Suenaga K, Rourke JP, York SJ, Sloan J (2009) ACS Nano 3:2547. doi:10.1021/nn900694t
11. Jiang G, Lin Z, Chen Ch, Zhu L, Chang Q, Wang N et al (2011) Carbon 49:2693. doi:10.1016/j.carbon.2011.02.059
12. Liang Y, Wang H, Casalongue HS, Chen Z, Dai H (2010) Nano Res 3:701. doi:10.1007/s12274-010-0033-5
13. Zhang Y, Ch Pan (2011) J Mater Sci 46:2622. doi:10.1007/s10853-010-5116-x
14. Marcano DC, Kosynkin DV, Berlin JM, Sinitskii A, Sun Z, Slesarev A, Alemany LB, Lu W, Tour JM (2010) ACS Nano 4:4806. doi:10.1021/nn1006368
15. Ni Z, Wang Y, Yu T, Shen Z (2008) Nano Res 1:273. doi:10.1007/s12274-008-8036-1
16. Ferrari AC (2007) Solid State Commun 143:47. doi:10.1016/j.ssc.2007.03.052
17. Ferrari AC, Robertson J (2000) Phys Rev B 61:14095. doi:10.1103/PhysRevB.61.14095
18. Kudin KN, Ozbas B, Schniepp HC, Prud'homme RK, Aksay IA, Car R (2007) Nano Lett 8:36. doi:10.1021/nl071822y
19. Ferrari AC, Meyer JC, Scardaci V, Casiraghi C, Lazzeri M, Mauri F et al (2006) PRL 97:187401. doi:10.1103/PhysRevLett.97.187401
20. Choi HC, Jung YM, Kim SB (2004) Korean Chem Soc 25:426
21. Thamaphat K, Limsuvan P, Ngotawornchai B (2008) Kasetsart Nat (J Sci) 42(5):357
22. Lazar G, Zellamaa K, Vascan I, Stamate M, Lazar I, Rusu I (2005) J Optoelectr Adv Mat 7:647
23. Wang G, Wang B, Park J, Yang J, Shen X, Yao J (2009) Carbon 47:68. doi:10.1016/j.carbon.2008.09.002
24. Kumar PM, Badrinarayanan S, Sastry M (2000) Thin Solid Films 358:122. doi:10.1016/S0040-6090(99)00722-1
25. Merouani A, Amardjia-Adnani H (2008) Int Sci J Altern Energy Ecol 6:152
26. Zielińska B, Borowiak-Palen E, Kalenczuk RJ (2011) J Phys Chem Solids 72:117. doi:10.1016/j.jpcs.2010.11.007
27. Yuan Z, Jia J, Zhang L (2002) Mater Chem Phys 73:323. doi:10.1016/S0254-0584(01)00373-X
28. Ahmed S, Rasul MG, Martens WN, Brown R, Hashib MA (2010) Desalination 261:3. doi:10.1016/j.desal.2010.04.062